

# Infrared absorption change in single-walled carbon nanotubes observed by combination spectroscopy of synchrotron radiation and laser

Junpei Azuma,<sup>a\*</sup> Minoru Itoh,<sup>b</sup> Masahiro Koike,<sup>b</sup> Masao Kamada<sup>a</sup> and Morinobu Endo<sup>b</sup>

<sup>a</sup>Synchrotron Light Application Center, Saga University, Honjo 1, Saga 840-8502, Japan, and

<sup>b</sup>Faculty of Engineering, Shinshu University, Nagano 380-8553, Japan.

E-mail: azuma@cc.saga-u.ac.jp

The Drude tail due to photo-excited carriers in single-walled carbon nanotubes (SWNTs) has been observed in the mid-infrared region by using combination spectroscopy of synchrotron radiation and Ti:sapphire laser. It is found that the density of photo-excited carriers increases as the sample temperature is raised from 12 to 300 K, and their lifetime is of the order of minutes at 300 K. These facts suggest that the movement of photo-excited carriers is largely affected by some extrinsic defect, thus resulting in the long-lasting Drude reflection in SWNTs.

© 2006 International Union of Crystallography  
Printed in Great Britain – all rights reserved

**Keywords:** SWNT; photo-excited carrier; synchrotron-radiation–laser combined experiment; IR; Drude tail.

## 1. Introduction

Since their discovery (Oberlin *et al.*, 1976; Iijima, 1991), carbon nanotubes have attracted much attention because of their one-dimensional property that the graphene sheets are rolled up as a tube with a nanoscale diameter. The development of the sample synthesis of single-walled carbon nanotubes (SWNTs) has allowed us to perform detailed experimental studies of the electronic structure. SWNTs have two electrical characters, semiconducting and metallic, depending on their diameter and chirality (Blasé *et al.*, 1994; Mintmire & White, 1995). Anomalous electronic density-of-states described by Tomonaga–Luttinger theory for one-dimensional systems has been reported for metallic SWNTs from conductance (Bockrath *et al.*, 1999) and photoemission (Ishii *et al.*, 2003) measurements. Discrete electronic structures peculiar to low-dimensional systems have also been revealed by infrared (IR) absorption measurements using a conventional globar lamp (Kataura *et al.*, 1999; Ichida *et al.*, 1999). It is essentially important to obtain information about the photo-excited carriers in semiconducting SWNTs, not only for basic research but also for applications of SWNTs.

Attractive pump–probe techniques using IR synchrotron pulse and laser pulse have been developed for the study of photocarrier dynamics (Lobo *et al.*, 2002; Carr, 2003). Such combination spectroscopy is a powerful tool because synchrotron radiation has high brightness in the IR region, in addition to the pulsed and broadband properties. Therefore, we have applied combination spectroscopy of synchrotron radiation and laser to the investigation of photo-induced IR

absorption changes in SWNTs in the spectral region between 500 and 15000  $\text{cm}^{-1}$ .

## 2. Experimental

The present measurements were conducted at the IR beamline BL-6A1 of the UVSOR facility of the Institute for Molecular Science, Okazaki, Japan. Fig. 1 shows the experimental set-up for pump–probe measurements. A Michelson interferometer (Bruker IFS-66V) was operated in rapid-scan

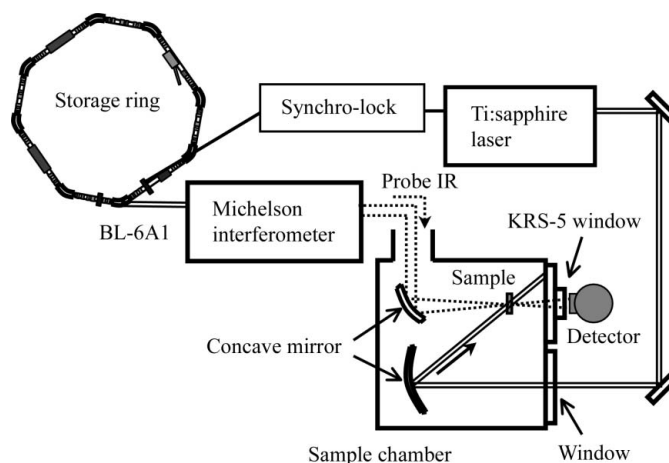


**Figure 1**  
Experimental set-up for pump–probe measurements using laser and synchrotron radiation. Asynchronous laser-induced absorption measurements can also be performed using this set-up without a Synchro-lock system.

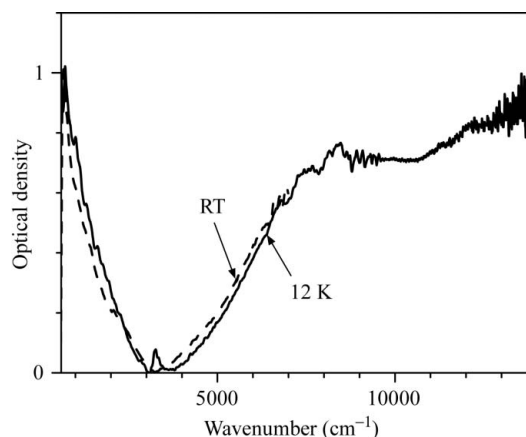
mode. Two beam splitters, quartz and KBr, were selected to cover the spectral ranges  $2500\text{--}15000\text{ cm}^{-1}$  and  $400\text{--}8000\text{ cm}^{-1}$ , respectively. These beam splitters can be changed in a few minutes by breaking the vacuum of the interferometer, which is separated from the sample chamber by a diamond window in terms of vacuum sections. An HgCdTe photoconductive detector and a Si photodiode were used in the IR ( $400\text{--}13000\text{ cm}^{-1}$ ) and visible ( $13000\text{--}15000\text{ cm}^{-1}$ ) regions, respectively, in combination with a KRS-5 window. Far-IR ( $80\text{--}700\text{ cm}^{-1}$ ) pump-probe measurements are also possible at this beamline by using a polyethylene window and a Si bolometer.

Photo-excitation was performed using a Ti:sapphire laser (Coherent, Mira-900F) at  $800\text{ nm}$  with an average power of  $300\text{ mW}$ . The laser-induced absorption change was obtained from the negative logarithm of the IR transmission spectra with laser irradiation divided by that without laser irradiation. The laser light pulse could be synchronized with the synchrotron radiation pulse by using a synchronization system (Coherent, Synchro-lock). This system allowed pump-probe measurements with laser light as pump and synchrotron radiation as probe. Asynchronous laser-induced absorption measurements were also available without using the Synchro-lock system. A time resolution of about  $1\text{ ns}$  was mainly determined by the pulse duration of the synchrotron radiation. The laser pulse duration was stretched to  $0.5\text{ ns}$  by an optical fiber of length  $50\text{ m}$ , which was used to deliver the laser light from the laser booth to the end-station of BL-6A1. The time delay in the pump-probe measurements was controlled electronically by the Synchro-lock system in the range  $0\text{--}11\text{ ns}$ . The maximum time range of  $11\text{ ns}$  was determined by the interval between successive synchrotron radiation pulses from bunched electrons in the storage ring. The time origin of the probe pulse was determined by checking the temporal overlap of a laser pulse and an unmonochromatized synchrotron radiation pulse using a photomultiplier (Hamamatsu, R7400U) placed at the sample position.

The SWNTs grown by the high-pressure carbon monoxide (HiPco) method were purchased from Carbon Nanotechnologies. Since the SWNTs delivered from the manufacturer contained about  $15\text{ wt\%}$  of Fe impurities, from the catalyst, they were purified by removing metal particles *via* air oxidation and HCl treatment. The purified SWNTs were dispersed in ethanol by ultrasonication. The samples used in the present experiment were prepared by misting the dispersed SWNTs onto  $\text{BaF}_2$  substrates which are transparent in the energy range above  $500\text{ cm}^{-1}$ . This limited the spectral region measurable in this study.

### 3. Results and discussion

Fig. 2 shows absorption spectra of SWNTs at  $12\text{ K}$  and at room temperature (RT). The band-to-band transitions from the valence band to the first- and second-lowest conduction bands in semiconducting SWNTs are clearly observed at around  $8000$  and  $13000\text{ cm}^{-1}$ , respectively. From a comparison with the IR data by Kataura *et al.* (1999), the diameter of SWNTs



**Figure 2** IR absorption spectra of SWNTs at  $12\text{ K}$  (solid line) and at RT (broken line).

used in this experiment is estimated to be about  $0.8\text{ nm}$ , which is consistent with the value reported by the manufacturer. The Drude tail from metallic SWNTs is also seen below  $3000\text{ cm}^{-1}$ . Its intensity is slightly enhanced at  $12\text{ K}$  compared with that at RT.

Transient bleaching and its ultrafast decay of a few ps have been reported for the first and second absorption band by degenerate pump-probe measurements using an optical parametric amplifier (Lauret *et al.*, 2003; Korovyanko *et al.*, 2004; Huang *et al.*, 2004). The results have been explained by assuming that most photo-excited carriers in SWNTs are relaxed to the ground state in a few ps through intrinsic relaxation processes. We first carried out pump-probe measurements at  $12\text{ K}$  and RT by using ns-pulsed synchrotron radiation and laser. Laser-induced changes of the IR absorption spectra were observed as a piled-up component under excitation at the second absorption band, but no significant temporal change was found in the time range from  $0$  to  $11\text{ ns}$ . Non-existence of temporal change is quite natural because the intrinsic relaxation of photo-excited carriers is completed within sub-nanoseconds.

For the next step, we focused the piled-up component of the laser-induced absorption change. Asynchronous laser-induced absorption change was obtained under laser excitation after sufficient exposure time of  $5\text{ min}$ . The results obtained at  $12\text{ K}$  and RT are presented in Fig. 3. One can see that an additional absorption tail appears below  $1000\text{ cm}^{-1}$ . This spectral change disappeared in several minutes after the laser excitation was stopped, indicating that the laser-induced change is not due to the sample damage. This additional absorption tail has a different spectral shape from the Drude tail due to metallic SWNTs. This means that the laser-induced spectral change in Fig. 3 is neither caused by the laser heating of metallic SWNTs nor the charge transfer from semiconducting SWNTs through the inter-tube coupling between SWNT bundles (Huang *et al.*, 2004). Fig. 3 also shows that the laser-induced change becomes greater at RT than at  $12\text{ K}$ .

Solid lines in Fig. 3 show the fitting results obtained by assuming that the reflection loss takes place by free carriers in

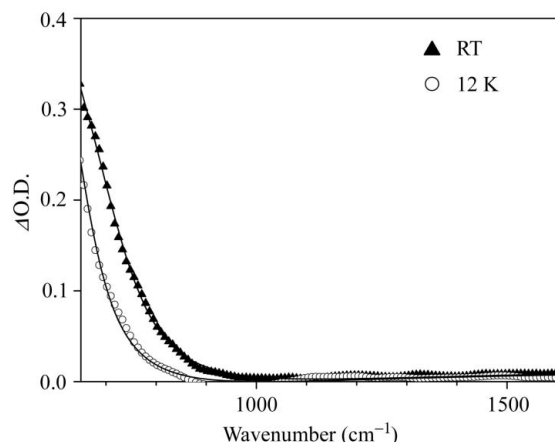


**Figure 3** Laser-induced absorption change in SWNTs at 12 K (open circles) and RT (black triangles). Solid lines are the best fit of the Drude formula to the experimental data points.

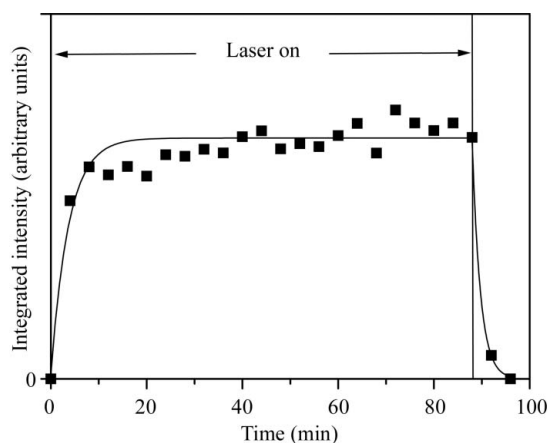


**Figure 4** Time evolution of the laser-induced absorption at RT. The solid line is a guide to eye.

the regime of the Drude model, which is expressed by the usual formula,

$$\epsilon(\omega) = \epsilon_{\infty} - \frac{\omega_p^2}{\omega(\omega + i\gamma)}. \quad (1)$$

The fitting is satisfactorily good, indicating that the additional Drude-like tail is ascribed to photo-excited carriers with a plasma frequency which is different from that of metallic SWNTs. The plasma frequency  $\omega_p$  and the damping rate  $\gamma$  are estimated as  $\omega_p = 2.0 \times 10^{13}$  Hz and  $\gamma = 3.3 \times 10^{12}$  Hz at 12 K and  $\omega_p = 2.2 \times 10^{13}$  Hz and  $\gamma = 5.1 \times 10^{12}$  Hz at RT. From the present results it is understood that the photo-excited carrier density and the damping rate increase with increasing temperature.

Time evolution of the laser-induced Drude tail at RT is shown in Fig. 4. The ordinate indicates the integrated intensity of this tail in the region above  $650 \text{ cm}^{-1}$ . The rise and decay with a time constant of a few minutes are observed at the start and the end of the laser irradiation, respectively. Such rise and decay were not found at 12 K, suggesting that the lifetime of photo-excited carriers decreases at low temperatures. This is

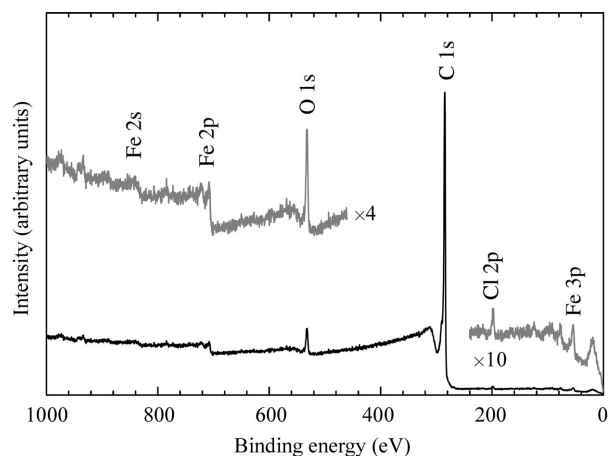


**Figure 5** XPS spectrum of SWNTs at RT.

consistent with the fitting analysis (Fig. 3) by the Drude model, in which the photo-excited carrier density related to the plasma frequency becomes greater at RT than at 12 K. However, it is difficult to explain the long lifetime of a few minutes in a framework of the dynamical behaviour of intrinsic photo-excited carriers. We suppose that the laser-induced Drude tail in Fig. 3 is ascribed to photo-excited carriers of extrinsic nature.

Commercial SWNTs before purification contain 15 wt% Fe catalytic ions as mentioned in §2. Fig. 5 shows the result of X-ray photoemission spectroscopy (XPS) for the purified SWNT samples that we used. Core levels of Fe impurities are observed at 55, 710 and 840 eV. This indicates that Fe impurities are still included even in the purified samples. The concentration of Fe impurity is estimated to be 10 wt% by taking into account the photoemission intensity and the photoionization cross section (Yeh & Lindau, 1985). It is thus reasonable to suppose that the remaining Fe impurities or the vacancies left by removing metal particles during the purification process should act as trap centers for electrons or holes. The same commercial samples are widely used to investigate optical and electrical properties of SWNTs (Korovyanko *et al.*, 2004; Huang *et al.*, 2004), but the existence of impurities or defects has not been noticed as a serious problem.

Further detailed studies of the temperature dependence and sample dependence are necessary to check the role of Fe impurities for the movement of photo-excited carriers in semiconducting SWNTs. Far-IR pump-probe experiments on samples without using BaF<sub>2</sub> substrate might help to obtain more information about the laser-induced absorption changes.

#### 4. Conclusion

We have observed the laser-induced IR absorption change of SWNTs by using a combination experiment of synchrotron radiation and Ti:sapphire laser. This laser-induced change has been ascribed to the Drude tail resulting from photo-excited carriers in semiconducting SWNTs. The intensity of the laser-induced Drude tail increases as the sample temperature is raised. It is likely that, at high temperatures, photo-excited

carriers become long-lived due to the repetition of the trapping and detrapping processes, enhancing the laser-induced Drude tail.

The authors are grateful to Professor Yoong Ahm Kim for help with the sample preparation. This work was supported by the Joint Studies Program (2002–2003) of UVSOR of the Institute for Molecular Science and also by the CLUSTER of the Ministry of Education, Culture, Sports, Science and Technology of Japan.

## References

- Blasé, X., Benedict, L. X., Shirley, E. L. & Louie, S. G. (1994). *Phys. Rev. Lett.* **72**, 1878–1881.
- Bockrath, M., Cobden, D. H., Lu, J., Rinzler, A. G., Smalley, R. E., Balents, L. & McEuen, P. L. (1999). *Nature (London)*, **397**, 598–601.
- Carr, G. L. (2003). *Nucl. Instrum. Methods*, **B199**, 323–327.
- Huang, L., Pedrosa, H. N. & Krauss, T. D. (2004). *Phys. Rev. Lett.* **93**, 017403.
- Ichida, M., Mizuno, S., Tani, Y., Saito, Y. & Nakamura, A. (1999). *J. Phys. Soc. Jpn.* **68**, 3131–3133.
- Iijima, S. (1991). *Nature (London)*, **354**, 56–58.
- Ishii, H., Kataura, H., Shiozawa, H., Yoshioka, H., Otsubo, H., Takayama, Y., Miyahara, T., Suzuki, S., Achiba, Y., Nakatake, M., Narimura, T., Higashiguchi, M., Shimada, K., Namatame, H. & Taniguchi, M. (2003). *Nature (London)*, **426**, 540–544.
- Kataura, H., Kumazawa, Y., Maniwa, Y., Umezumi, I., Suzuki, S., Ohtsuki, Y. & Achiba, Y. (1999). *Synth. Metals*, **103**, 2555–2558.
- Korovyanko, O. J., Sheng, C.-X., Vardeny, Z. V., Dalton, A. B. & Baughman, R. H. (2004). *Phys. Rev. Lett.* **92**, 017403.
- Lauret, J.-S., Voisin, C., Cassabois, G., Delalande, C., Roussignol, Ph., Jost, O. & Capes, L. (2003). *Phys. Rev. Lett.* **90**, 057404.
- Lobo, R. P. S. M., LaVeigne, J. D., Reitze, D. H., Tanner, D. B. & Carr, G. L. (2002). *Rev. Sci. Instrum.* **73**, 1–10.
- Mintmire, J. W. & White, C. T. (1995). *Carbon*, **33**, 893–902.
- Oberlin, A., Endo, M. & Koyama, T. (1976). *J. Cryst. Growth*, **32**, 335–349.
- Yeh, J. J. & Lindau, I. (1985). *Atom. Data Nucl. Tables*, **32**, 1–155.